MEASUREMENT OF CROSS-CONTAMINATION BETWEEN VEHICLES USING SCALE MODELS

S. B. Riffat and R. Clarke
Building Technology Group
Department of Architecture and Planning
University of Nottingham
University Park
Nottingham
NG7 2RD
United Kingdom

Abstract

This paper deals with the problem of exhaust cross-contamination between vehicles in a slow-moving traffic queue, as would be found in a busy modern city. This study has been undertaken using a open-jet wind tunnel, to determine the level of exhaust contamination around a 1:10 scale model car under various prevailing wind conditions. Tracer-gas techniques have been combined with static pressure measurements, to model the flow of pollutants around a vehicle body. Analysis of experimental data has shown that high concentrations of pollutants are present around the front, and in the lee of a vehicle in slow moving traffic.

Notation

C_m	Measured level of pollutant (ppm)
C_p	Pressure coefficient (dimensionless)
C_s	Pollutant level at source (ppm)
d	Displacement height (0 in smooth terrain) (m)
I_i	i-component of turbulence intensity
i'	Fluctuating component of velocity
k	von Karmen's constant (0.4)

U	Mean tunnel velocity (m/s)
U_z	Mean velocity at height z (m/s)
U_*	Friction velocity (m/s)
z	Height (m)
z_0	Roughness length (m)
ΔP	Static pressure difference (Pa)
α	Pollutant fraction (%)
ρ	Density of air (kg/m^3)
σ_i	Standard deviation of the i-component of turbulence intensity at height z

1. INTRODUCTION

Air pollution caused by vehicle emission is a problem in many cities in the U.K. Driver and passenger exposure to vehicle emissions including volatile compounds (VOCs), carbon monoxide (CO), ozone (O_3), nitrogen oxides ($NO/N_2O/NO_x$), is of increasing concern and studies have shown that exposure to these compounds results in 1000-5000 additional cancer deaths per year.[1] Asthma and other chronic respiratory diseases can also be directly linked to vehicular pollution, and have shown marked increases in the last decade. Vehicle drivers are also exposed to particles (atmospheric or vehicle originated) and pollens, which are also of considerable health concern. Most investigations of sick building syndrome (SBS) have ignored the fact that people commuting to work are exposed to high levels of pollutants whilst travelling.[2] There is a lack of information regarding the extent of driver exposure to pollutants, factors affecting exposure, and the link between exposure during commuting and SBS.

Links between SBS and exhaust pollution cannot be lightly dismissed, as the main pollutants found in vehicle exhaust can cause most of the recorded symptoms of SBS.

Exposure to carbon monoxide (CO) for example causes nausea and headaches, and if combined with a poor working environment could promote more disturbing symptoms. This study is part of a project which aims to quantify levels of pollutants present around a vehicle, while travelling in various traffic conditions.

The concentration of pollutants within vehicles is directly influenced by ventilation conditions within the vehicle, (eg, vent closed and air conditioning on, windows closed, and vent open etc.). For example in urban driving, cross-contamination between vehicles via air ventilation systems is responsible for driver exposure to high levels of pollutants. An extensive literature search has been carried out and this showed that very little research has been conducted on pollution within vehicles. Petersen and Sabersky [3] have measured carbon monoxide, ozone and nitrogen oxides inside automobiles driven in Los Angeles during summer months. Hayes [2] measured ozone concentration within vehicles and found that vehicle speed affects the infiltration rate and ozone levels. Chan et.al [1] measured the driver's exposure to organic compounds for different traffic patterns. Heinsohn et.al [4] used a sequential box model to predict the instantaneous contaminant concentration, eg., cigarette smoke in an automobile passenger compartment. However, these studies did not consider the relationship between ventilation rate and pollutant distribution within vehicles nor pollutant cross-contamination between vehicles.

2. THEORY

To simplify the interpretation of tracer-gas data, the measured quantity is expressed as a ratio known as the pollutant fraction (equation 1).

Where α is the dimensionless pollutant fraction, Cm is the measured level of pollutant

$$\alpha = \frac{Cm}{Cs} \times 100 \qquad (1)$$

(ppm) and Cs is the level of pollutant measured at the source (ppm). Pressure data are treated in a similar manner, in that a dimensionless quantity is used to express a change from the ambient pressure (equation 2).

$$Cp = \frac{\Delta P}{\frac{1}{2}\rho U^2} \qquad (2)$$

Where Cp is the pressure coefficient, ΔP is the measured static pressure (Pa), ρ is the density of air (nominally 1.2kg/m^3), and U is the mean tunnel speed (m/s).

The tunnel velocity profile was determined using a model of a thermally neutral atmosphere [6] (equation 3).

$$U_z = \left(\frac{U_*}{k}\right) \ln\left[\frac{(z-d)}{z_0}\right] \qquad (3)$$

And the turbulence intensity was measured (equation 4).

$$I_i = \frac{(i')^{\frac{1}{2}}}{U_z} = \frac{\sigma_i}{U_z} \qquad (4)$$

(A typical value of I_i for low urban terrain would be around 0.4 near the ground decreasing to 0.2 at approximately 70m height.)

3. EXPERIMENTAL WORK

3.1 Low Velocity Atmospheric Wind Tunnel

The tunnel used for this series of tests was based on a small open-jet wind tunnel developed for teaching by the Building Research Establishment (B.R.E.).[6] This tunnel has a maximum flow rate of 4.5m/s and a working section of 1.0m wide by 0.75m high and 2.25m long (Figure 1). Two layers of honeycomb are fitted in the bellmouth to straighten the incoming flow, and are followed by a 0.5mm mesh screen. Following the entry section there is a 0.75m settling chamber to allow disturbances caused by the honeycomb and screen to decay, and to allow means to be introduced to modify the flow profile. Between the working section and the fan is a transformer to change the 1.0m x 0.75m cross section to a suitable shape for the fan mounting. The entry to the transformer is larger than the settling chamber exit, to allow for some expansion of the flow through the working section. Fan speed is controlled using a variable auto-transformer to vary the voltage applied to the 'squirrel cage' drive motor.

The tunnel was measured to determine any velocity variations across the tunnel section. Two sets of data were recorded; the first measured 0.5m downstream of the settling chamber, the second 1.5m downstream of the settling chamber. Only negligible velocity variations were found at both positions ($\pm$3%), although the turbulence intensity was higher at the second. The flow down the tunnel was found to be stable up to 200mm from the edge of the table, beyond this point some marked decreases in speed and an increase in turbulence intensity were noted. After the initial tests a velocity profile grid was fitted, which gave an exponential profile to the tunnel flow.

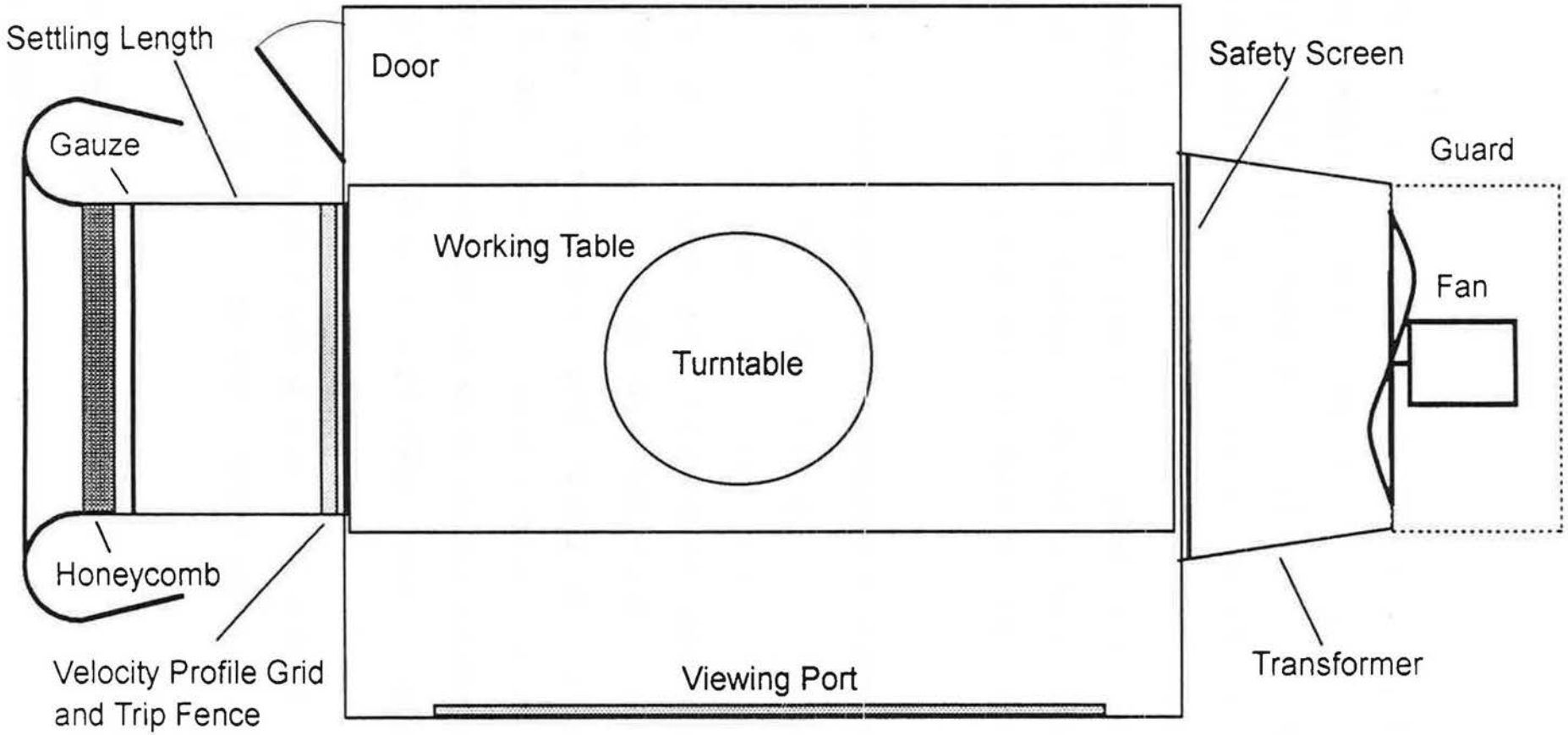

Figure 1. Layout of the low speed wind tunnel.

A trip fence fitted just beyond the velocity profile grid was used to increase the turbulence intensity, although the short working section of the tunnel made accurate modelling of turbulence difficult. With the fence fitted the turbulence intensity was 0.25 (25%), 20mm above the table, falling to 0.01 (1%) at 500mm (U= 4.5m/s).

3.2 Wind Tunnel Models

Two hollow model cars were constructed using 10mm MDF, at a scale of 1:10 (Figure 2). The models were for simplicity, only representations of a full scale car and no attempt was made to model detail. One car (A) was fitted with a single injection tube to simulate the engine exhaust. This was of a size (1.0mm ID) to allow simulation of the measured flow of gas from a car, whilst the engine was idling (15-20m/s). The second model (B) was fitted with twenty-three static pressure tappings, to allow measurement of gas concentrations and pressure around the body. These tappings were machined from 0.8mm ID brass tubing, and fitted on all of the body surfaces. PVC tubing was then fed through the tunnel turntable to allow connection of the model to the instrumentation.

3.3 Instrumentation

Sixteen of the model pressure tappings were connected to a Furness Controls FC091 selection box. Tappings were connected in pairs to allow pressure and gas-concentration measurements to take place simultaneously. Gas analysis was carried out using a Binos 1000 gas analyzer and the pressure measurements were made using a Furness Controls micro-manometer. All of the instrumentation was connected to a Datron 1055 data logging system controlled by a portable P.C. (Figure 3).

The tracer-gas constant-injection system consisted of a pump with a flow rate of 1l/min, a mixing reservoir, and a Brandenburg mass flow controller. This system was adjusted to give a tracer-gas concentration of $5x10^5$ppm measured at the exhaust outlet of model A. Pollutant fraction could then be calculated for the model B pressure tappings.

Smoke visualisation tests were conducted using a Elven Precision model FVSP204 smoke generator fitted with a hand-held probe.

4 RESULTS AND DISCUSSION

A model was first tested to see that the airflow around the body was similar to that of a typical car. To accurately model a flow around a model in a wind tunnel the Reynolds number (Re) of the model should match that of the full-scale version. To do this the tunnel speed would have to be increased by ten times. Fortunately bluff bodies (sharp edged objects) are not greatly affected by differences in Re, and so for this study Re has been ignored.

Two models were then placed on the wind tunnel turntable 120mm apart, for the pressure and gas concentration tests. The spacing of the models was chosen to simulate slow moving city traffic and would be 1.2m at full scale. Sets of data were recorded at three tunnel speeds (4.5m/s, 3.0m/s and 1.5m/s) at 15° increments from 0° to 90°.

the model , with a increase in static pressure toward the rear of the model, on the leeward side. This corresponds with flow around a typical car and is as expected. Analysis of the data again showed the influence of the windscreen, with a decrease in static pressure below the point where the windscreen meets the bonnet on the leeward side of the model and a corresponding increase on the windward side (Tappings 7 and 8).

Conclusions

The high pollutant levels found on the front and bonnet pressure tappings could significantly increase pollution levels within the vehicle cabin. Placement of air inlets at these two positions is common and more research would seem to be needed to determine more suitable placing. Measured data show that significant negative pressures are present on the leeward side of the model, this corresponds to the presence of high concentrations of pollutant.

Model testing has shown that the levels of pollutants around the front of a car can rise considerably at low speeds. The results highlighted the importance of the location of vehicle vents if cross-contamination between vehicles is to be minimised. For example, it may be possible to site a vent at a location which has a low pollutant concentration for any wind direction. This study indicates a need for further research into vehicle ventilation and pollutant distribution.

With the models facing directly into the wind a corridor of pollutant was recorded along the right hand side of model B (Figure 4). Smoke was used to show the plume and confirmed the tracer measurements with dense smoke present over the right hand third of the model. Tracer-gas concentrations were found to be very high between the two models at most wind directions, with up to 1% of the emitted tracer being drawn into the tappings on the front of the model (tappings 1 and 2) at low tunnel speeds. High concentrations of tracer were also found at the tappings to the rear of the bonnet (tappings 3 and 4), although these were more heavily influenced by the wind direction. Figures 5 and 6 show the calculated pollutant fraction present at these tappings.

Pollutant concentrations were found to fall sharply on the windward side of the model, with increase of wind angle. While the concentration of pollutant was found to remain at significant levels on the leeward side of the model until a wind angle of 75° (Figure 7). Concentrations of tracer were also found to be significant on the rear of model B (Figure 8), with concentrations of 0.5% present at shallow wind angles. At all wind angles the concentration of tracer across the rear of the model evenly distributed. with only small variations of concentration occuring. With the tunnel running at a velocity of 1.5m/s, a flow of pollutant was observed to go beneath the model causing a increase in pollutant level at the rear (tappings 15 and 16). In general the concentration of pollutant gradually fell toward the rear of the model. with a slight increase below the angle of the windscreen caused by tracer flowing over the bonnet (Figures 4, 9, 10 and 11). Smoke visualisation tests confirmed the flow of tracer-gas around the model, with high concentrations of smoke being visible across the bonnet and in the lee of the car (Figure 12).

Pressure coefficients were also calculated for model B. The measurements showed that there is a gradual decrease in static pressure toward the rear of the windward side of

References

1 Chan, C. C., Özkaynak, H., Spengler, J.D. & Sheldon, L., Driver exposure to volatile organic compounds, CO, Ozone and NO_2 under different driving conditions. *Environ. Sci. Technol.* **25**(1991) 964-972

2 Hayes, S. R., Estimating the effect of being indoors on total personal exposure to outdoor air pollution. *J. Air Pollut. Cont. Assoc.* **39**(1989) 1453-1461

3 Peterson, G. A. & Sabersky, R. H., Measurement of pollutant inside an automobile. *J. Air Pollut. Cont. Assoc.* **25**(1975) 1028-1033

4 Heisohn, R. J., O'Donnell, W. R. & Tao, J., Automobile passenger car ventilation. *Trans.* ASHRAE **99**(1993) Pt.2

5 Bauman, F. S., Ernest, D. R. & Arens, E. A., Wind pressure distribution on long building rows in urban surroundings. *Trans* ASHRAE **94**(1988) Pt.2

6 Sexton, D. E. A simple wind tunnel for studying airflow around buildings. *Architect and Building News* (1968) 983-985

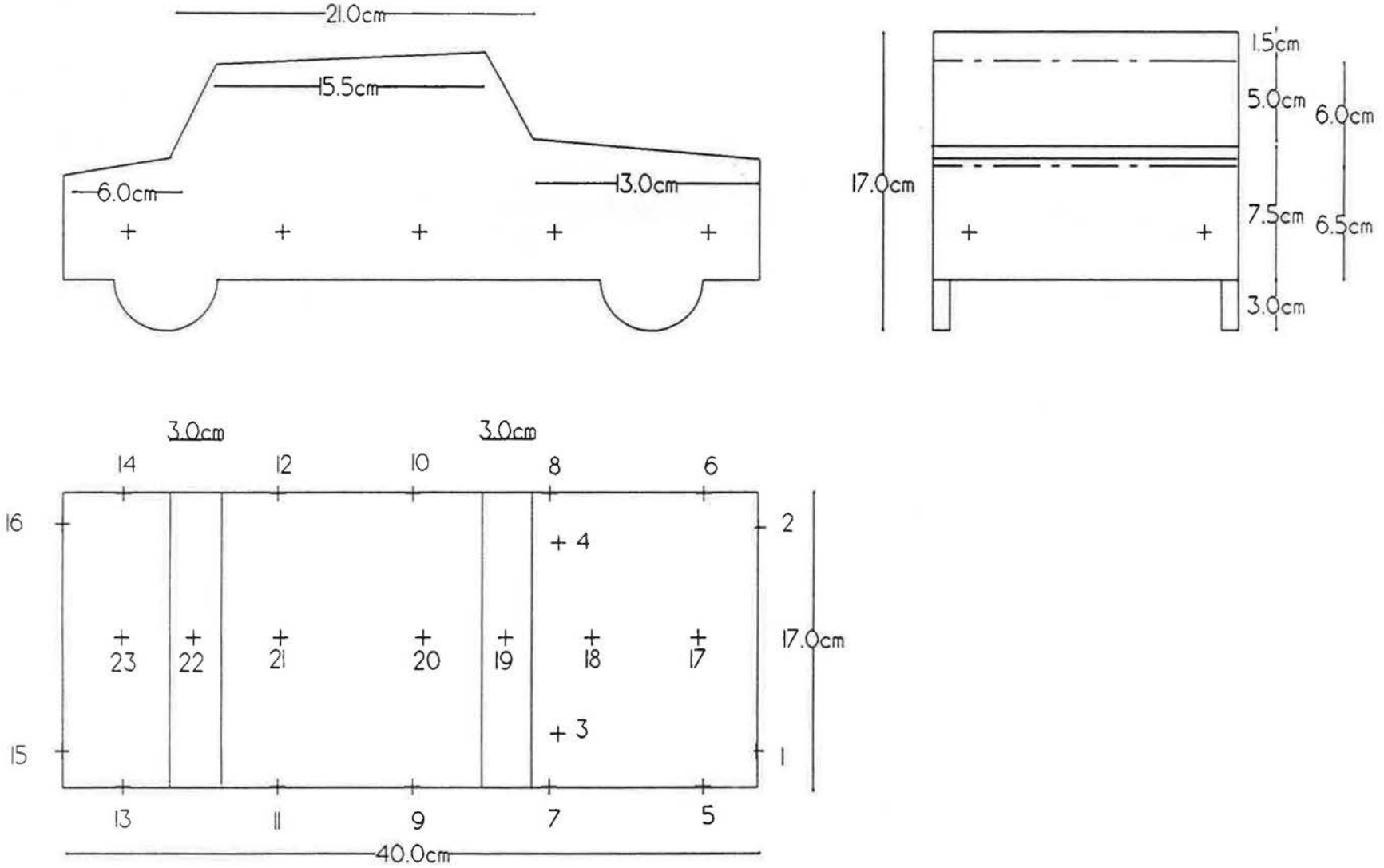

Figure 2. Model car used for cross contamination tests, showing the locations of the pressure tappings.

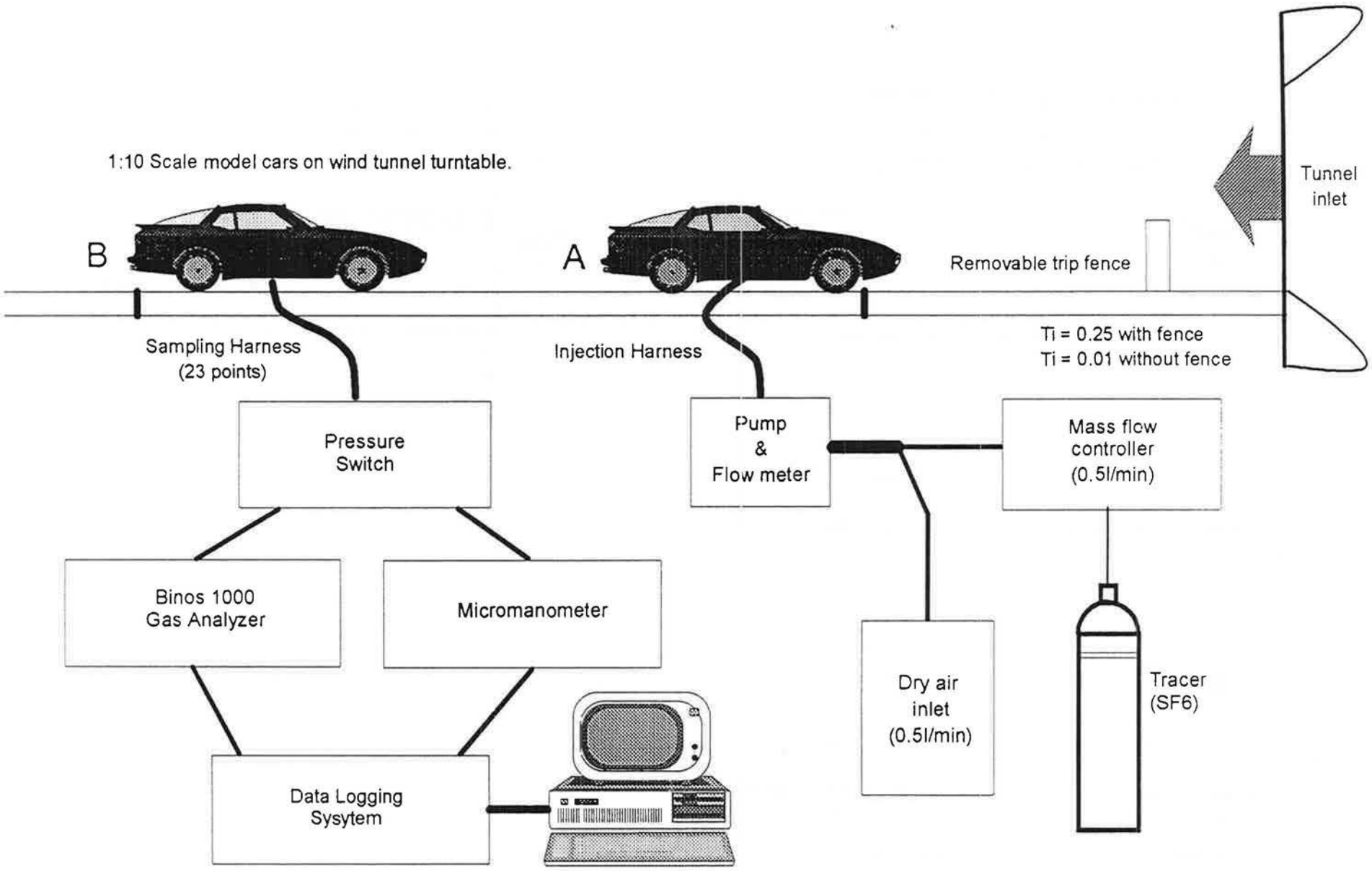

Figure 3. Layout diagram of apparatus used to measure cross contamination.

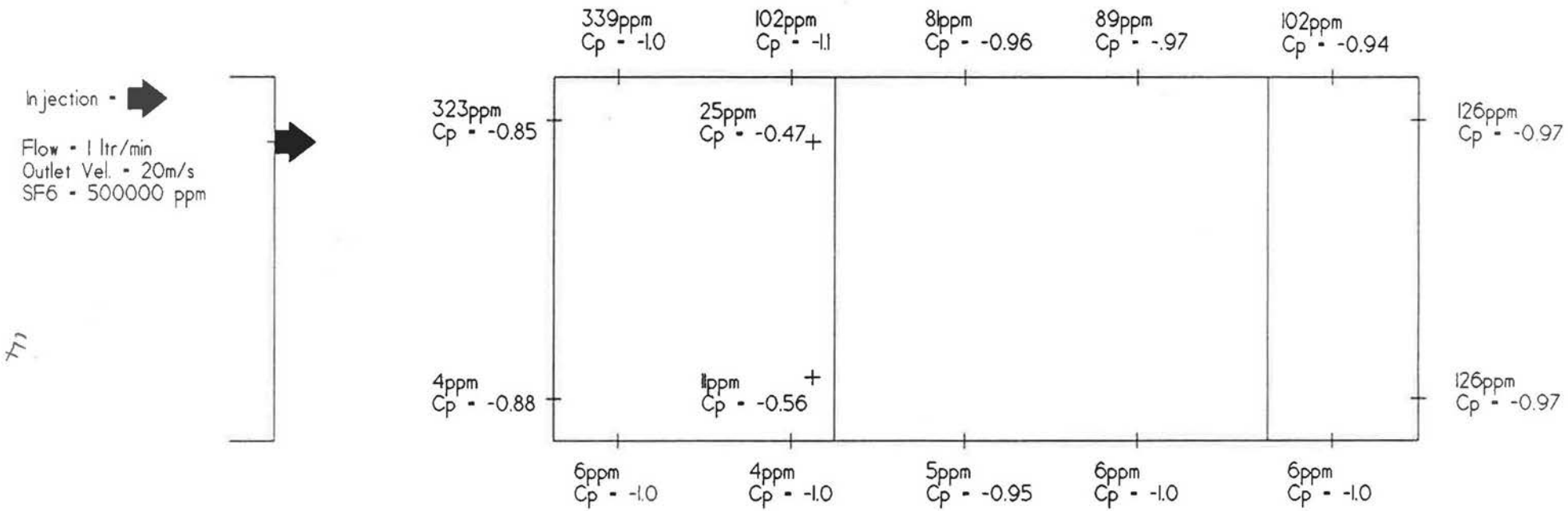

Figure 4. C_p and SF_6 concentration at 0° yaw (Tunnel speed 4.5 m/s).

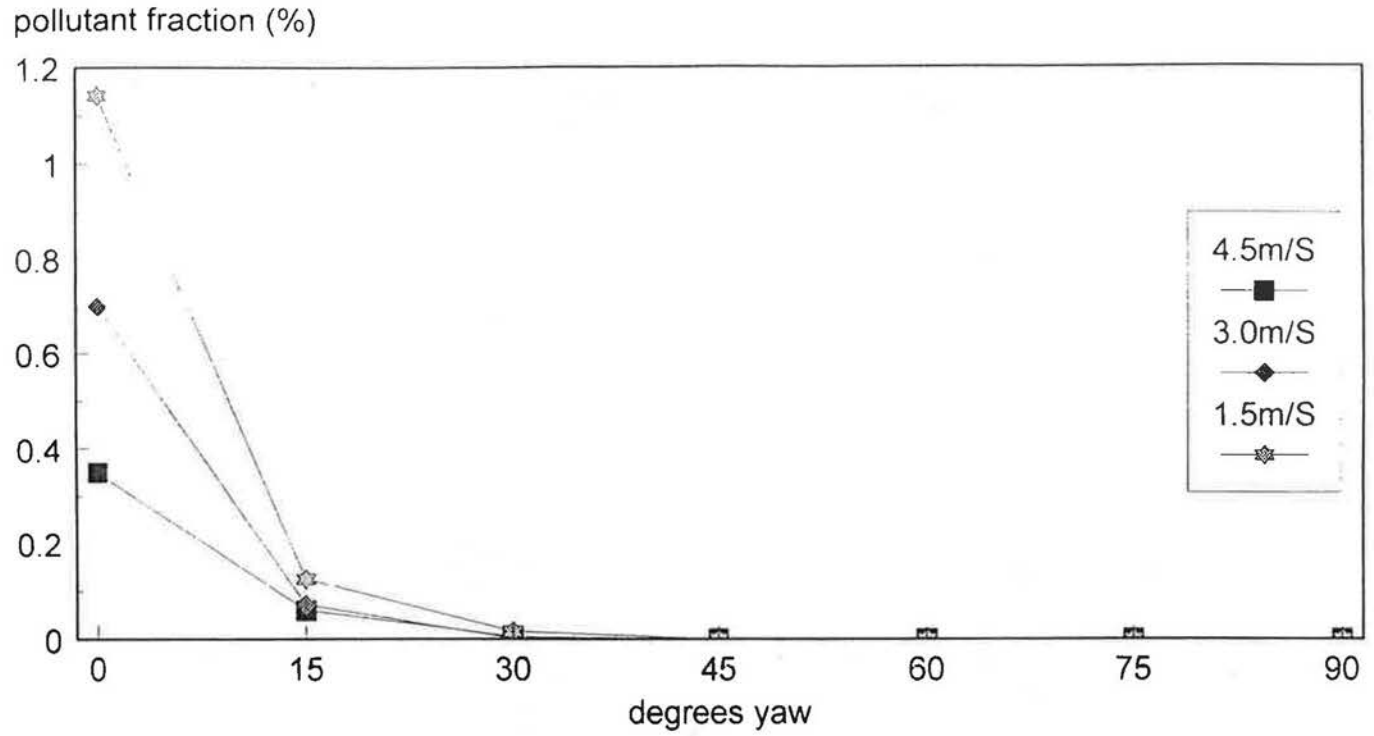

Figure 5a. Pollutant present on pressure tapping number 1

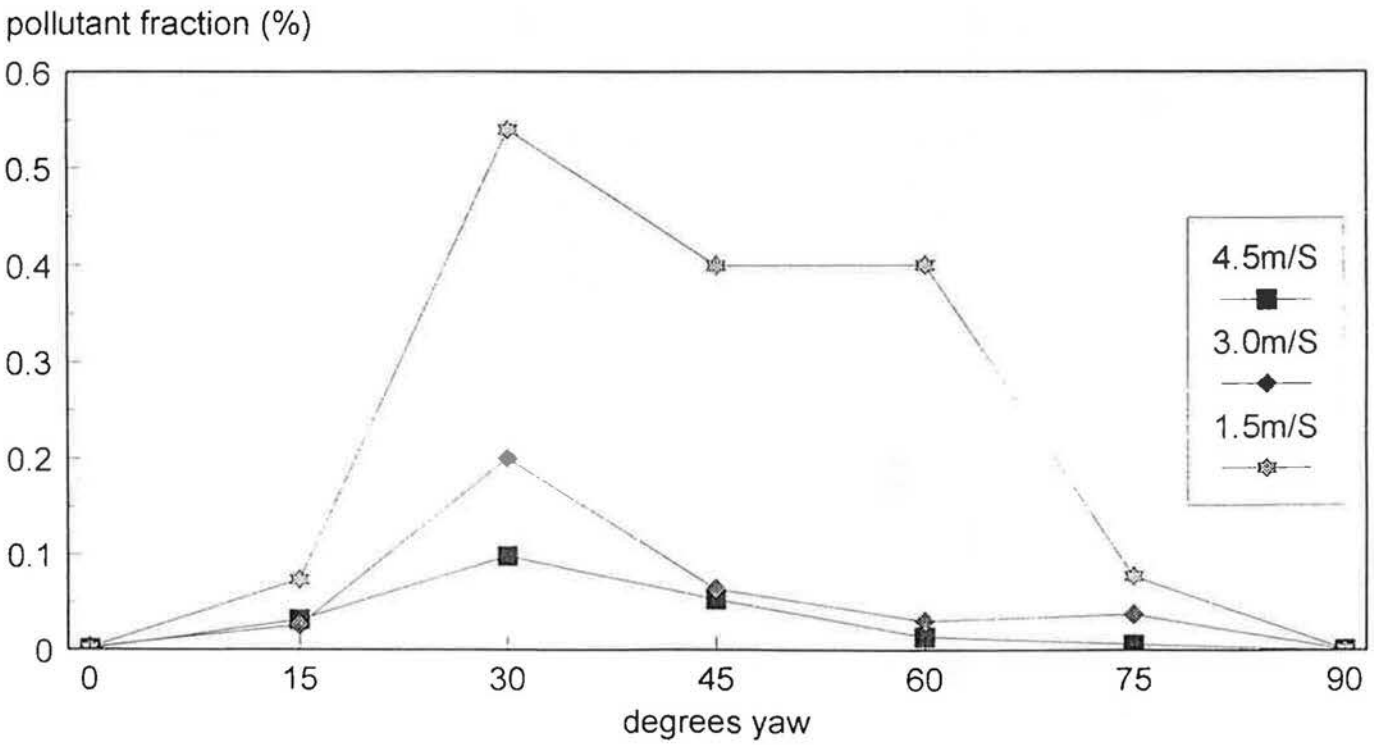

Figure 5b. Pollutant present on pressure tapping number 2

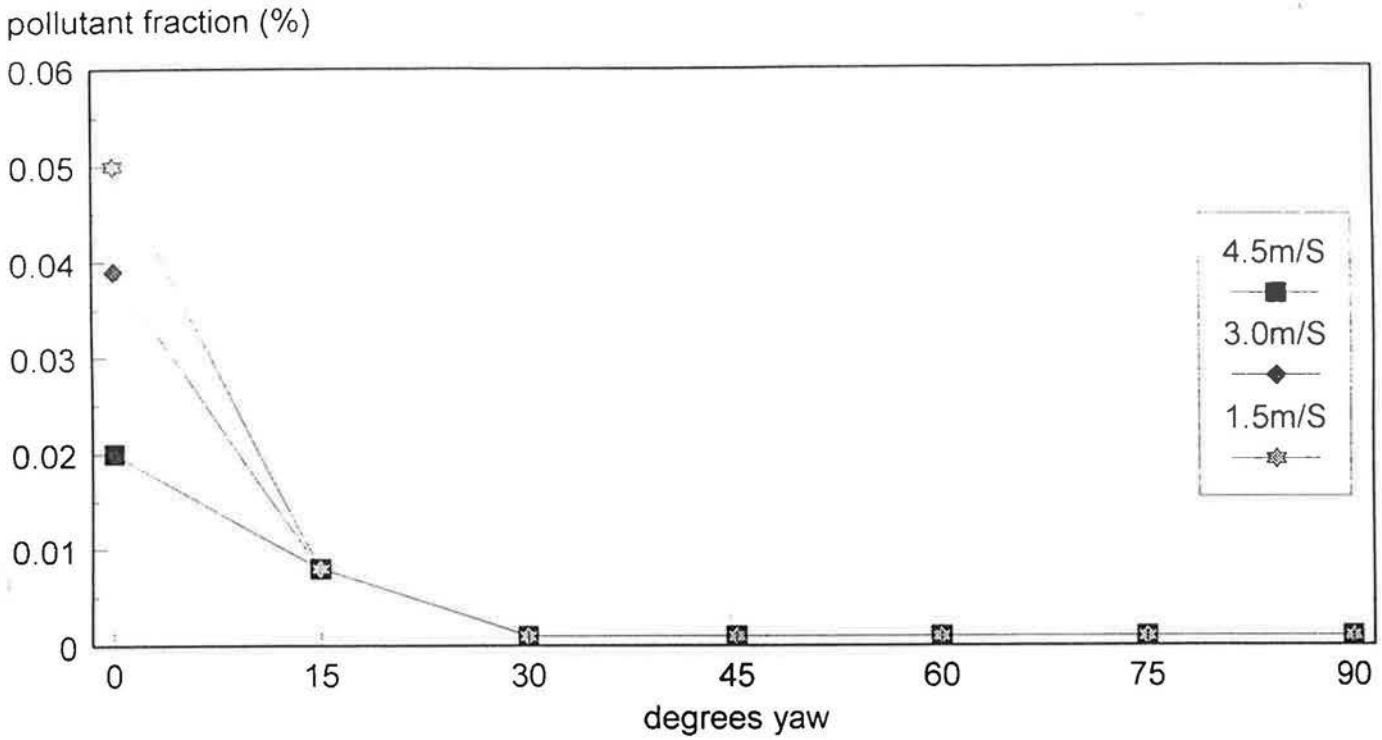

Figure 7a. Pollutant present on pressure tapping number 7.

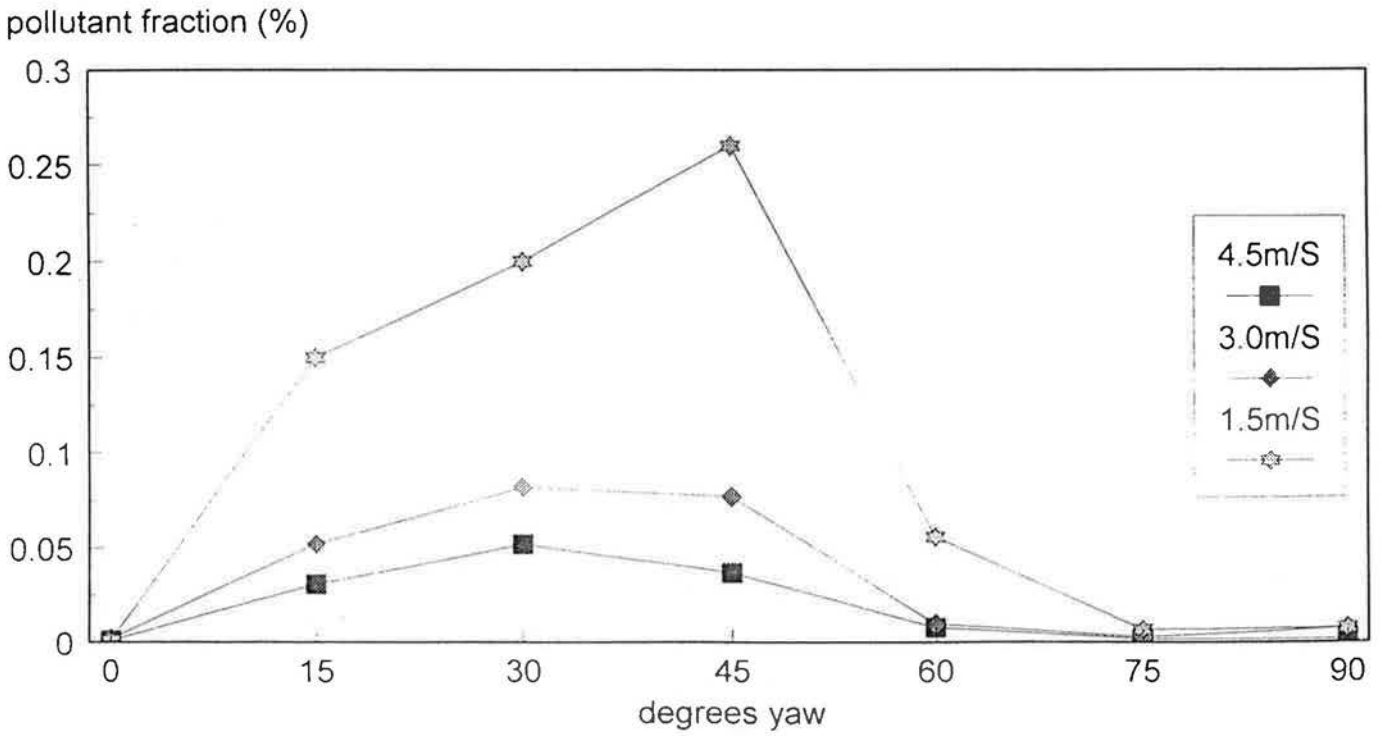

Figure 7b Pollutant present on pressure tapping number 8

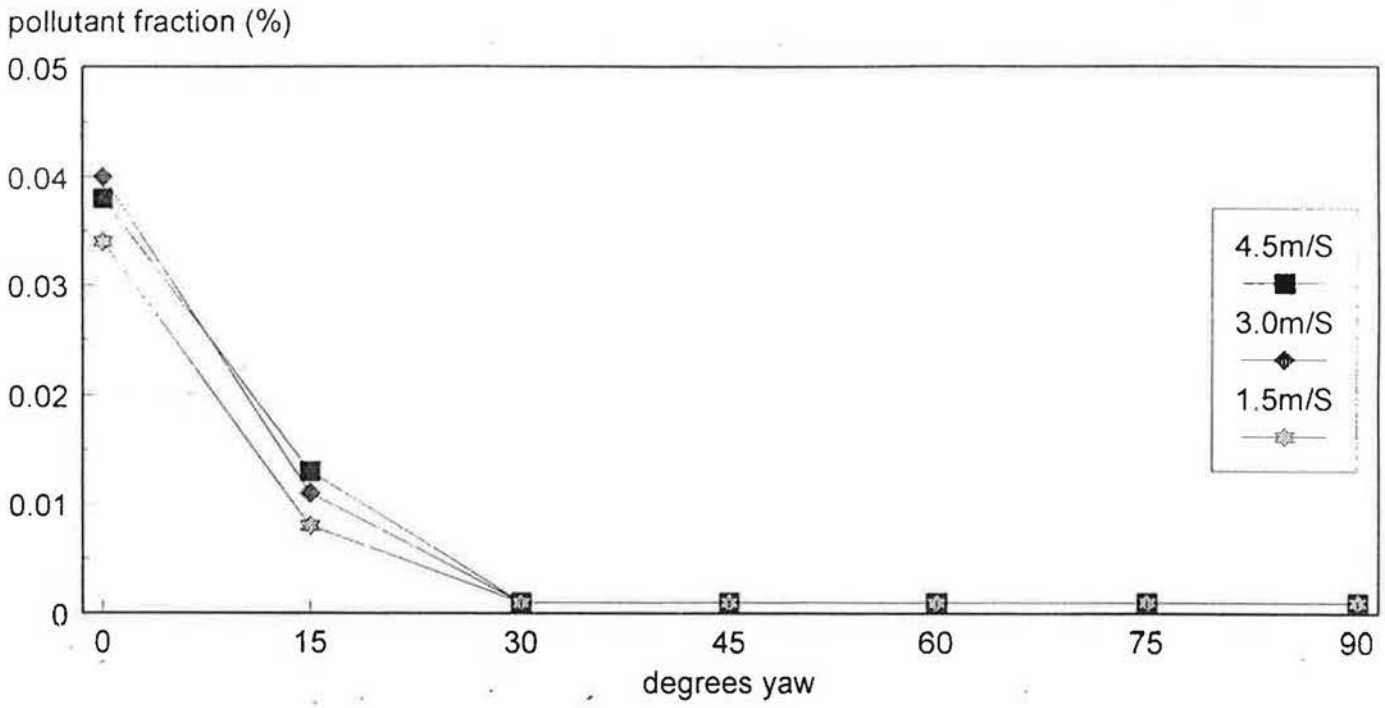

Figure 6a. Pollutant present on pressure tapping number 3.

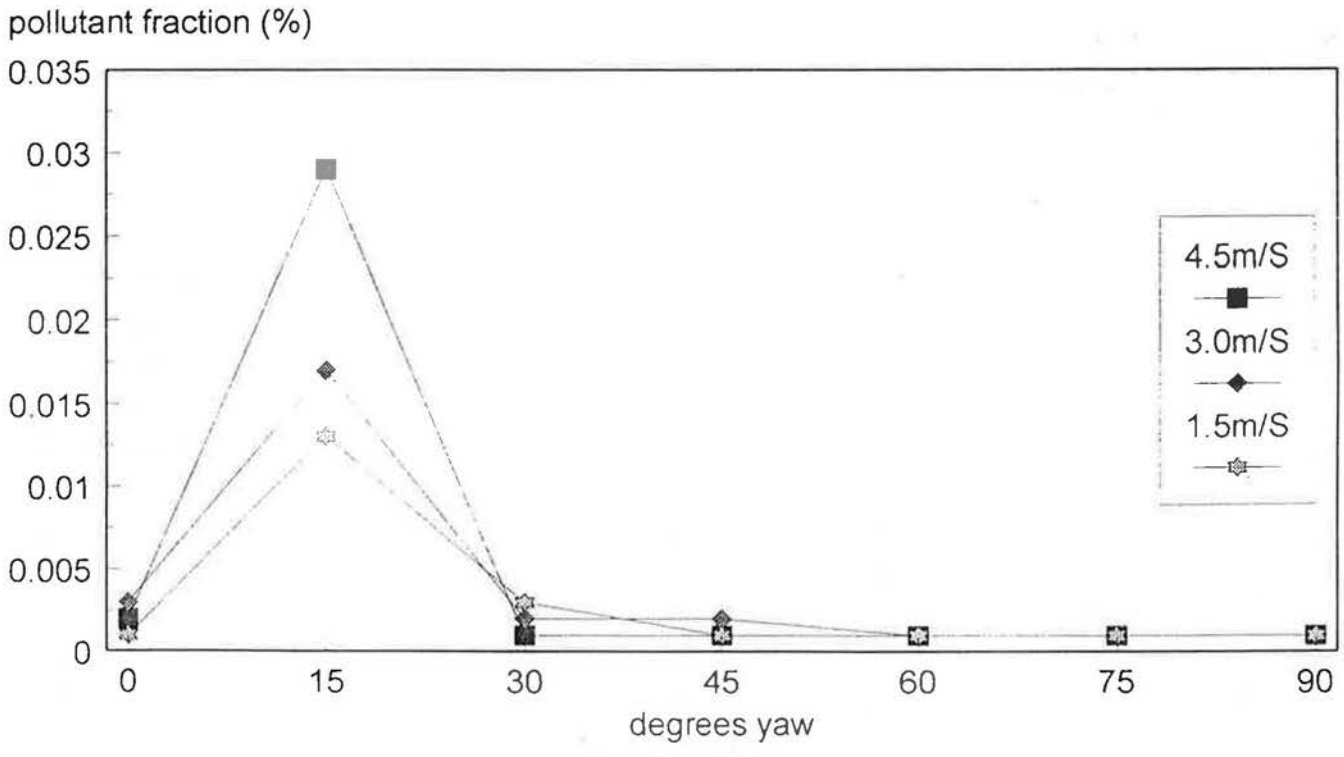

Figure 6b Pollutant present on pressure tapping number 4

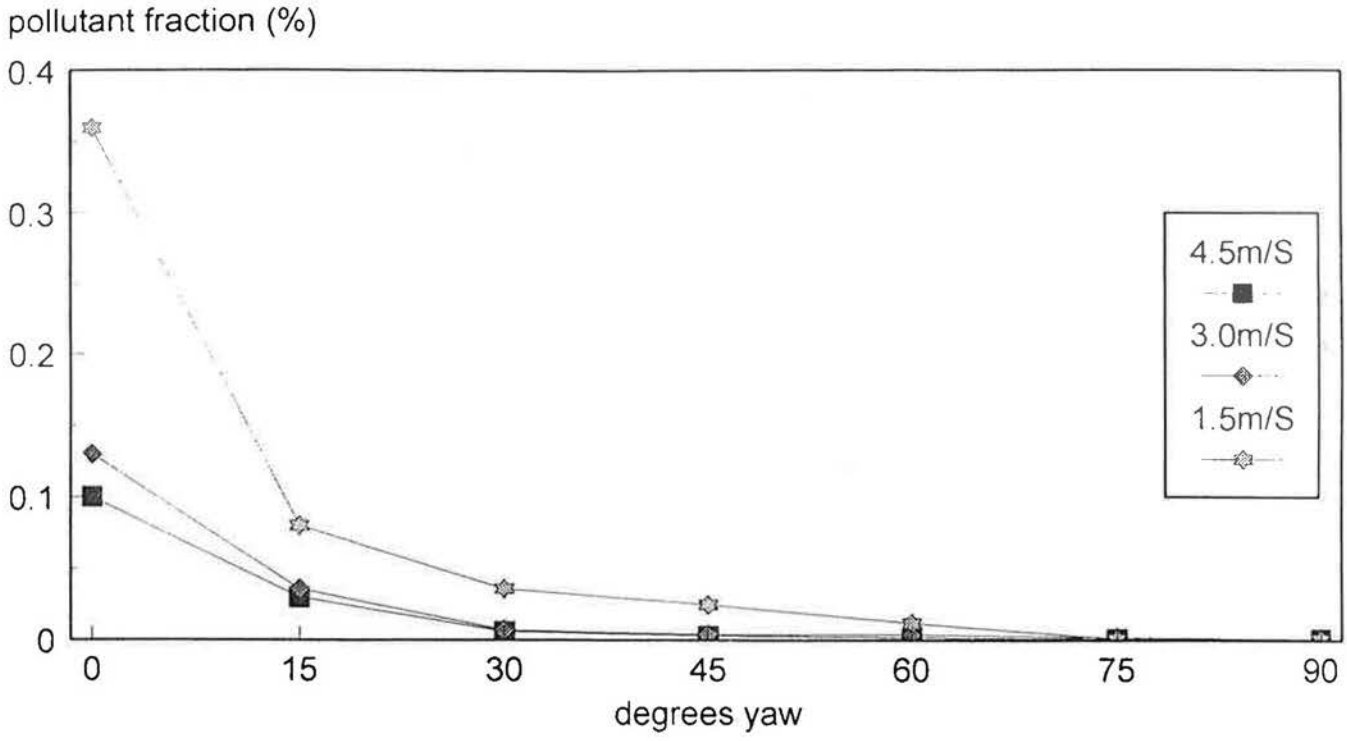

Figure 8a. Pollutant present on pressure tapping number 15.

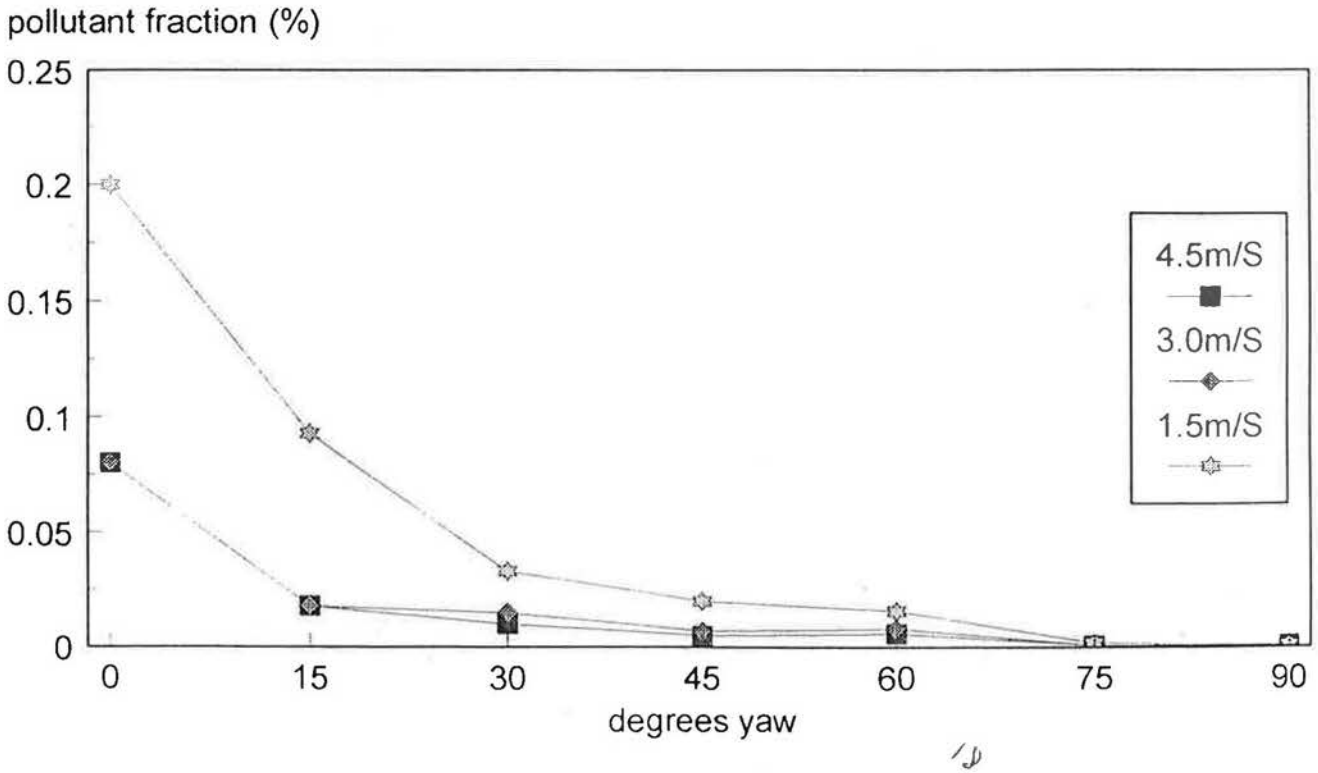

Figure 8b Pollutant present on pressure tapping number 16

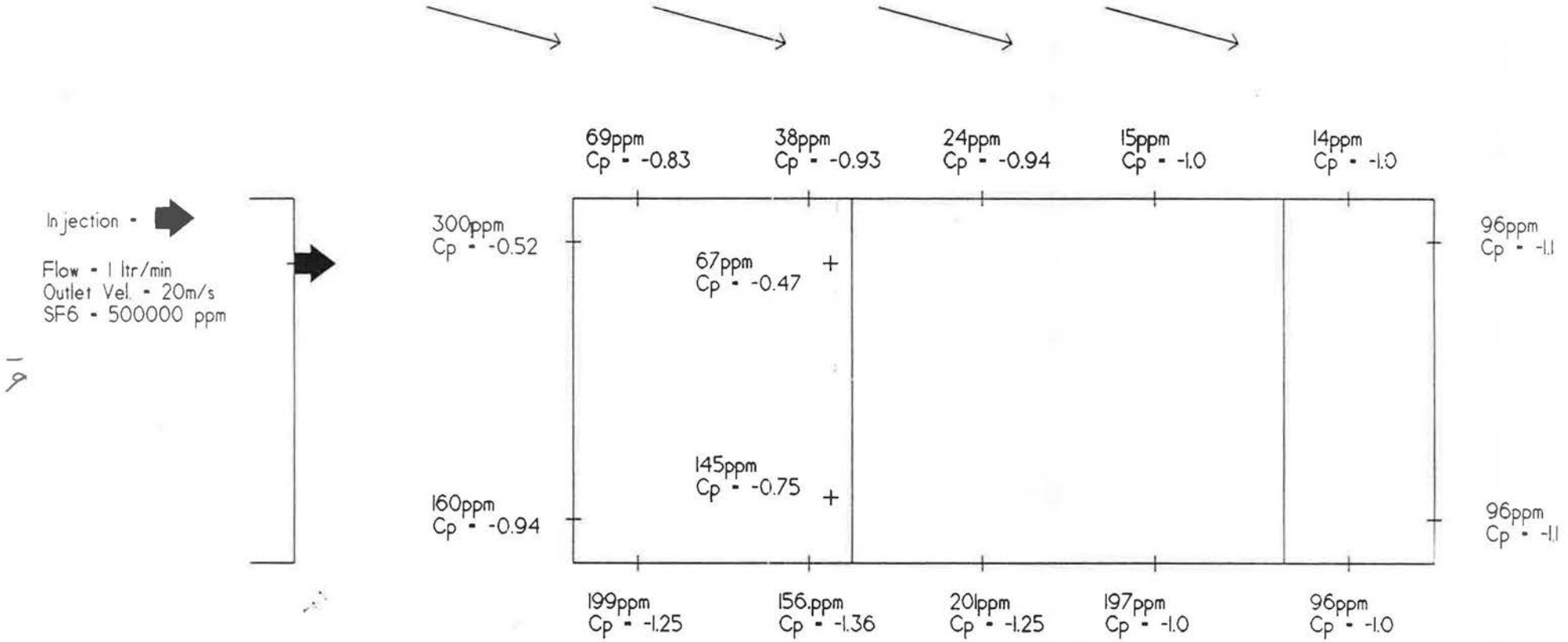

Figure 9. C_p and SF_6 concentration at 15°yaw (Tunnel speed 4.5 m/s).

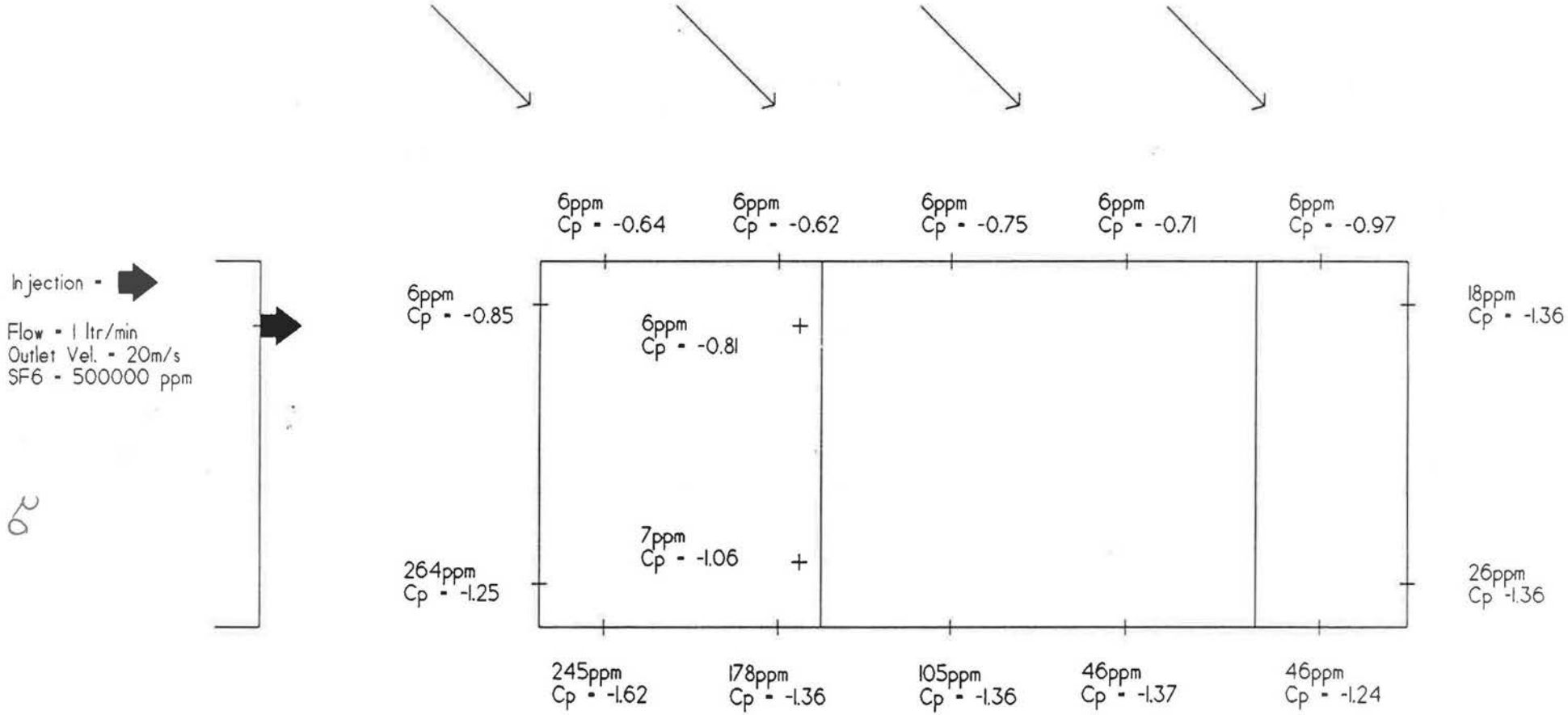

Figure 11. C_p and SF_6 concentration at 45°yaw (Tunnel speed 4.5 m/s).

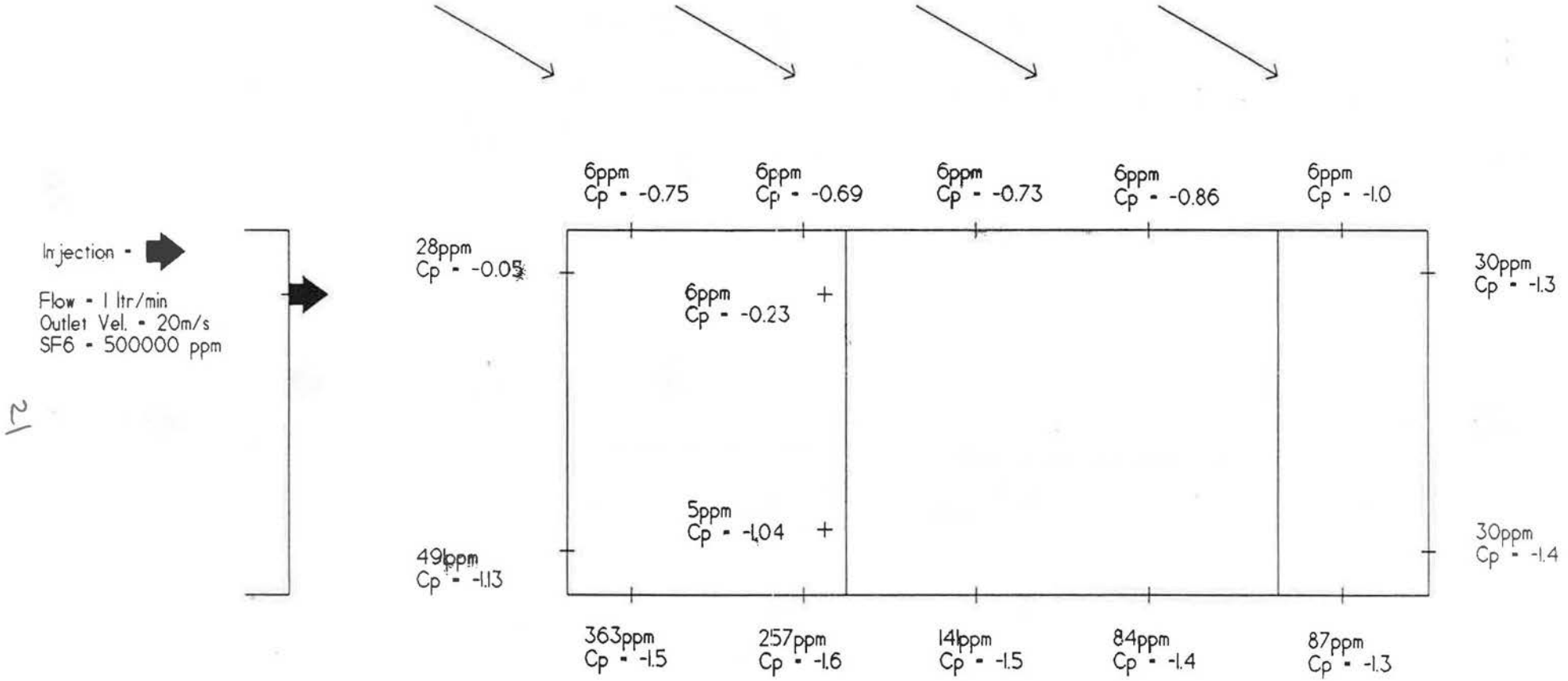

Figure 10. C_p and SF_6 concentration at 30°yaw (Tunnel speed 4.5 m/s).